Journal of Hazardous Materials 252–253 (2013) 204–212

Contents lists available at SciVerse ScienceDirect

Journal of Hazardous Materials

journal homepage: www.elsevier.com/locate/jhazmat

Reactivity screening of microscale zerovalent irons and iron sulfides towards different CAHs under standardized experimental conditions

Milica Velimirovic[a,b], Per-Olof Larsson[c], Queenie Simons[a], Leen Bastiaens[a,*]

[a] Flemish Institute for Technological Research (VITO), Boeretang 200, 2400, Mol, Belgium
[b] University of Antwerp, Department of Bio-Engineering, Groenenborgerlaan 171, 2020 Antwerp, Belgium
[c] Höganäs AB, Global Development, Bruksgatan 35, 26383, Sweden

HIGHLIGHTS

- Standardized test procedure for studying the reactivity of iron was developed.
- Degradation kinetic for 23 different iron based particles towards different CAHs.
- Comparing to nZVI, newly designed mZVIs showed promising reactivity properties.
- The biogenic iron sulfides were the least reactive iron based particles.

ARTICLE INFO

Article history:
Received 27 November 2012
Received in revised form 5 February 2013
Accepted 25 February 2013
Available online xxx

Keywords:
Zerovalent irons
Iron sulfides
CAHs remediation
Reactivity screening

ABSTRACT

A standardized batch test procedure was developed and used to evaluate the reactivity of twelve newly designed microscale zerovalent iron (mZVI) particles and two biogenic iron sulfides towards a mixture of chlorinated aliphatic hydrocarbons (CAHs) and their breakdown products. For comparison, commercially available mZVIs, nanoscale zerovalent irons (nZVIs), iron sulfides (FeS) and granular zerovalent iron were also tested. Reactivity of the particles was based on observed (k_{obs}) and mass normalized (k_M) pseudo-first-order degradation rate constants, as well as specific surface area normalized reaction rate constants (k_{SA}). Sorption characteristics of the particles were based on mass balance data. Among the new mZVIs, significant differences in reactivity were observed and the most reactive particles were identified. Based on k_M data, nZVI degraded the examined contaminants one to two orders of magnitude faster than the mZVIs. k_M values for biogenic iron sulfides were similar to the least reactive mZVIs. On the other hand, comparison of k_{SA} data revealed that the reactivity of some newly designed mZVIs was similar to highly reactive nZVIs, and even up to one order of magnitude higher. k_{SA} values for biogenic iron sulfides were one to two orders of magnitude lower than those reported for reactive mZVIs.

1. Introduction

Zerovalent iron (ZVI) has been widely used for site remediation by permeable reactive barriers (PRBs) because of its passive character, low cost, availability and high ability to dehalogenate chlorinated aliphatic hydrocarbons (CAHs) over wide concentration ranges [1–3]. Mostly, granular sized ZVIs have been used in PRBs [4]. In respect to fine injectable ZVI particles for in situ remediation of CAHs, mainly nanoscale zerovalent iron (nZVI) particles were studied because of their extreme reactivity, although their efficiency in the field is not completely clear [5,6]. Loss in reactivity and decreased mobility of uncoated nZVIs is explained by rapid aggregation and agglomeration forming micron sized aggregates [7]. In comparison with the nanoscale ones, microscale zerovalent iron (mZVI) particles are less expensive, have a longer lifetime and pose less risk for human health [8–10]. The capacity of soil mineral iron sulfide (FeS) to transform several CAHs has been reported by several research groups [11–15]. At least one study compared the reactivity of FeS with granular ZVIs [12]. However, no detailed study on comparison of FeS, mZVIs and nZVIs has been reported.

Comparison of mZVIs and nZVIs in respect to their efficiency for degrading chlorinated ethenes has been extensively reported [16–19]. Generally, mZVI particles remove CAHs slower than the same mass of well suspended nZVIs. The higher reactivity of nZVIs is explained by the greater specific surface area [16,20]. On the other hand, when focusing on surface area normalized reaction rate constants, similar reactivity is obtained for nZVIs and mZVIs [21]. Following the research of Mace [22], conducted to prove advantages

* Corresponding author. Tel.: +32 14 33 5634.
E-mail addresses: milica.velimirovic@vito.be (M. Velimirovic), Per-Olof.Larsson@hoganas.com (P.-O. Larsson), queenie.simons@vito.be (Q. Simons), leen.bastiaens@vito.be (L. Bastiaens).

0304-3894/$ – see front matter © 2013 Elsevier B.V. All rights reserved.
http://dx.doi.org/10.1016/j.jhazmat.2013.02.047

of nZVIs over microscale and bimetallic nanoscale iron particles, Comba et al. [23] collected 112 field case studies available in the literature where fine ZVIs were used for in situ remediation of CAHs. According to statistical analysis, a higher degree of CAHs degradation was observed for mZVIs than for nZVIs when the ZVI material is not combined with other technologies (e.g. addition of organic component, presence of a catalyst) [23].

A number of papers have been published focusing on the reactivity of different ZVI particles deduced from batch studies [16,19,24–29]. This resulted in a wide range of reactivity within ZVIs towards various CAHs. The characteristics of the iron material are an explanation, but also different experimental conditions (pH, buffer, temperature etc.), iron pretreatment kinetic and type of organic pollutants [30]. Additionally, many of these batch studies were limited to a single CAH-compound. Degradation of a mixture of contaminants has been generally reported in numerical experiments [31]. Consequently, large reactivity data sets using consistent experimental conditions for different iron based particles including iron sulfides and mixtures of different pollutants are limited.

The primary objective of the present study was to evaluate the reactivity of 23 different iron based fine particles towards a mixture of chlorinated ethenes and ethanes, using consistent experimental conditions. This paper focuses mainly on mZVI particles (17 materials, from which 12 newly designed) and biogenic iron sulfides (2 materials). One granular ZVI, one commercial FeS and two nZVIs were included as reference materials. In contrast to other studies, where batch and column experiments were mainly performed for one chlorinated aliphatic hydrocarbon [16,24,28,32–34], the study reported herein evaluates the reactivity of different iron based particles towards an environmentally relevant mixture of four chlorinated compounds: tetrachloroethene (PCE), trichloroethene (TCE), cis-dichloroethene (cDCE) and 1,1,1-trichloroethane (1,1,1-TCA) under standardized batch test conditions. The motivation behind using the selected standardized degradation procedure for a mixture of CAHs, was to compare the CAH-removal kinetics of newly designed mZVIs as well as biogenic iron sulfides with commercially available ZVI materials within a reasonable time frame and with a reasonable amount of effort. Mixtures of pollutants are also representative for most contaminated sites. The formation and degradation of breakdown products of the tested CAHs (i.e. 1,1-dichloroethane) was also considered, rendering information about the reactivity towards these compounds.

2. Materials and methods

2.1. Media

Artificial groundwater used for the batch tests consisted of anaerobic autoclaved MilliQ water supplemented with 0.5 mM $CaCl_2.2H_2O$, 0.5 mM $MgCl_2.6H_2O$, 0.5 mM $NaHCO_3$ and 0.5 mM $KHCO_3$ [35]. Under anaerobic conditions, the pH was adjusted to neutral by adding 1 M HCl and the artificial groundwater was spiked aiming at a final concentration of approximately 5 mg L^{-1} of PCE, TCE, cDCE and 1,1,1-TCA each. The chemicals PCE (> 99% purity), TCE (> 99%) and cDCE (97%) were supplied by Acros Organics (Belgium). 1,1,1-TCA (97%) was purchased from JT Baker Chemicals (The Netherlands).

2.2. Iron based particles

The reducing iron based particles included in the test comprise zerovalent irons (micron, nano and granular size) and iron sulfides. Details on size, specific surface area, supplier, production process of all the studied iron based particles are given in Table 1. Twelve mZVI types with different particle size distributions, morphologies and slightly different chemical compositions were prepared by Höganäs using two different production methods. The two biogenic iron sulfides were freshly produced at small scale by growing two different mixed enrichment cultures of sulfate-reducing bacteria in Postgate's medium B [36]. Biogenic iron sulfides were harvested by centrifugation at 4000 rpm for 10 min. at room temperature. The supernatant was discarded and the precipitates were used in degradation experiments. The final concentration of biogenic iron

Table 1
Properties of studied iron based particles.

Iron name	PSD [D_{10}, D_{50}, D_{90}][a] [μm]	BET[b] [$m^2\ g^{-1}$]	Production process	Supplied by	Form
FeA4[C]	300–1300 mm[c]	1.15	Granulated grey cast iron	Gotthart Maier (DE)	Iron Filings
FeH1[N]	8, 26, 50	0.27	Iron oxides	Höganäs (SE) [N]	Powder
FeH3[N]	36, 84, 168	0.06	Atomization		
FeH4[N]	22, 41, 62	0.09	Atomization		
FeH6[N]	41, 98, 162	0.09	Iron oxides		
FeH7[N]	44, 96, 158	0.12	Iron oxides		
FeH8[N]	34, 63, 97	0.35	Iron oxides		
FeH9[N]	3, 7, 16	0.50	Iron oxides		
FeH10[N]	9, 22, 42	1.21	Iron oxides		
FeH11[N]	6, 19, 38	3.98	Iron oxides		
FeH12[N]	6, 17, 32	3.62	Iron oxides		
FeH13[N]	7, 18, 34	1.50	Iron oxides		
FeH14[N]	21, 79, 162	11.40	Iron oxides		
FeQ2[C]	8, 26, 44	0.40	Iron oxides	Höganäs (SE)	Powder
MS200[C]	2.1, 4.2, 7.2	0.36	Carbonyl irons	BASF (DE)	Powder
MS200+[C]	1.7, 3.7, 7.1	0.47	Carbonyl irons		
SM[C]	1.4, 2.5, 4.1	0.48	Carbonyl irons		
HQ[C]	0.6, 1.2, 2.4	0.82	Carbonyl irons		
Nanofer25s[C]	$D_{50} < 0.05$[c]	25.0[c]	Surface modified nanoscale iron	NANOIRON (CZ)	Suspension
RNIP[C]	$D_{50} < 0.07$[c]	4.97	Fe^0/Fe_3O_4 core-shell nZVI particles	TODA (JP)	Suspension
FeS Aldrich[C]	12, 89, 268	0.90	Iron sulfides	Aldrich	Powder
FeS BIO1[N]	0.002-001[d]	3.40	Biogenic iron sulfides	VITO[N]	Suspension
FeS BIO2[N]	0.002-001[d]	3.40	Biogenic iron sulfides		

[a] Particle Size Distribution measured by laser diffraction with a Sympatec Helos/Rodos dry particle size analyzer.
[b] BET: Specific Surface Area analyzed with a Micromeritics Flowsorb II according to the Brunauer–Emmett–Teller (single point measurement).
[c] Producers data.
[d] According to Ohfuji and Rickard in Earth and Planetary Sc. Lett. 241 (2006) 227–233.
[N] Newly prepared for this study.
[C] Commercially available.

sulfides included in the tests was calculated via dry weight measurement and precipitation of organic matter.

2.3. Degradation experiments

Batch experiments were performed to study degradation of a mixture of CAHs by different iron based particles. Glass vials contained 50 g L^{-1} of granular or microscale ZVI, FeS, approximately 40 g L^{-1} of biogenic iron sulfides or 5 g L^{-1} of nZVI. Lower concentrations of nanoscale particles were used due to their high reactivity. Subsequently, 100 ml of anaerobic, artificially contaminated groundwater was added to the vials in an anaerobic glove box (nitrogen), leaving a 60 ml headspace. The bottles were capped with butyl/PFTE grey septa. The experiments were carried out in triplicates and at a groundwater temperature of 12 ± 1 ^{0}C. As the role of mass transport processes in determining degradation kinetics is very important, all vials were placed on an Edmund Bühler SM 30-control shaker (125 rpm/min). Each series included a control set without iron particles to identify losses of CAHs (e.g. photodegradation, adsorption, leakage, samplings). In the control sets, no formation of metabolites was observed and losses of the examined CAHs were ~ 10–15%. Mass transfer resistance at the vapor/liquid interface was not considered as these phases are assumed to be in equilibrium with each other [37]. As a function of time, the concentration of CAHs was followed along with pH and ORP values. For nanoscale particles, samples were taken 0, 3, 6, 8 and 22 days after the start of the test, for the other particles after 0, 14, 28, 49 and 105 days.

The concentrations of CAHs, intermediate- and end-products were determined via direct headspace measurements using a Varian GC-FID (CP-3800 with CTC-autosampler) equipped with a Rt-U plot column for the detection of ethene, ethane and acetylene or a split-splitless injector followed by a Rt-X column (Restek) and a DB-1 column (J&W Scientific) for analysis of CAHs. At each sampling time 1.5 ml of sample was removed for measurements of the oxidation-reduction potential (ORP) and pH using a redox/pH meter (Radiometer). Mass recoveries were made on molar basis (PCE + TCE + cDCE + VC + 1,1,1-TCA + 1,1-dichloroethane (1,1-DCA) + acetylene + ethene + ethane) to determine if sorption occurred. To determine acetic acid, diethyl ether extraction was used. Samples were analyzed by a Focus GC-FID, while the quantification was done according to the internal standard method. Based on triplicate analysis of samples, analytical errors were typically ~ 5%.

2.4. Data analysis

A pseudo-first-order model was applied to describe the reductive dechlorination of a parent compound by the reactive materials [24]:

$$C = C_0 e^{-k_{obs}t} \quad (1)$$

where C is the concentration at any time and C_0 is the initial concentration of parent compound (mg L^{-1}), k_{obs} is the pseudo-first-order rate constant (h^{-1}) and t (h) is the reaction time. The natural logarithmic transformation of eq. (1) yields a linear equation with the first-order rate constant k_{obs} as slope:

$$\ln(C/C_0) = -k_{obs}t \quad (2)$$

Mass normalized rate constants (k_M, L g^{-1} h^{-1}) and specific surface area normalized rate constants (k_{SA}, L m^{-2} h^{-1}) were calculated using the following relationship [21,24]:

$$k_{obs} = k_{M\rho M} = k_{SA} a_s \rho_M = k_{SA} \rho_a \quad (3)$$

with a_s as the specific surface area of iron based particles (m^2 g^{-1}), ρ_M as the mass concentration of the iron based particles (g L^{-1}) and ρ_a as the surface area concentration of iron based particles (m^2 L^{-1} of solution).

3. Results and discussion

Comparison of the CAH removal kinetics of different reactive iron based particles was based on observed (k_{obs}) and mass normalized (k_M) pseudo-first-order degradation rate constants, as well as specific surface area normalized reaction rate constants (k_{SA}) under similar experimental conditions. Disappearance rate curves of parent compound by the reactive materials are presented and discussed in detail in supporting information (SI1 and SI2). Generally, pseudo-first-order behavior was found predominant for most examined iron based particles. Exceptions were mainly related with sorption effects. The evolution of pH and redox potential during the test are summarized in SI3. On average, the pH increased rapidly above pH 9.9 ± 0.7 due to the iron corrosion [38], and remained constant afterwards.

3.1. CAH-removal efficiencies by different iron based particles

Data on selected pollutant removal efficiencies are given in Table 2. After 105 days, the granular iron (FeA4), used as a reference material in this study, degraded > 95% of PCE, TCE and 1,1,1-TCA and > 40% of cDCE. Nanofer25s, the most efficient iron among all examined iron based particles, removed 100% of the pollutants mixture within a 22 days reaction period. The most reactive mZVIs capable of PCE, TCE, cDCE and 1,1,1-TCA removal of > 98% within the test period (105 days) are: FeH4, FeH8, FeH14 and FeQ2. In contrast, the least reactive mZVI particles were FeH1 and FeH9. The observed fast pH increase from pH 7.20 to approximately 11 with no observed change in the redox potential shows the low reduction capacity of these particles. Possible explanations for this comprise inhibition of reactivity due to the high pH or passive film of iron oxides and/or iron-oxyhydroxides on the surface. pH values above 11 may be an indication for less reactive mZVI particles. The lowest pH (9.33) was observed for FeH3 and FeH4 which are both produced via atomization process where low amount of iron oxides on the iron surface is expected. At the end of the test period, FeS Aldrich removed 95% of TCE and 20% of cDCE, while complete degradation of PCE and 1,1,1-TCA was observed. Biogenic FeS BIO1 realized a slow degradation of PCE (37%) and 1,1,1-TCA (62%) after 105 days. However, FeS BIO2 was not reactive towards the examined CAHs. Moreover, 70% of all studied irons were capable of efficient removal of 1,1,1-TCA. Despite the high percentage of tested pollutants removal, the microscale particles FeH11 and FeH12 showed mainly sorption tendencies which was concluded from calculated mass recoveries (26–27%) and no increase of the degradation products (ethene and ethane) and no pressure build-up. Low calculated mass recoveries were also obtained for highly reactive materials such as nZVIs, HQ, FeH4 and FeH14, where high production of ethene and ethane and high pressure build-up were observed (data not shown). A loss of volatile reactants and products during the sampling process due to the high pressure build-up in batch reactors has also been observed by other researchers [3]. In addition, incomplete mass recoveries can be explained by the fast transformation of 1,1,1-TCA and formation of acetic acid as degradation end-product.

The PCE, TCE, cDCE and 1,1,1-TCA observed degradation rate constants (k_{obs}) are summarized in Table 3. The range in reported k_{obs} corresponds to half life time ($t_{1/2}$) from 6 h to 866 days, depending on the type of iron based particles used and the specific pollutant. Considering k_{obs} data, Nanofer25s, the iron with the highest surface area and tested in ten times lower concentration, is the

Table 2
Summary of results for PCE, TCE, cDCE and 1,1,1-TCA removal efficiency by studied iron based particles.

Treatment (concentration)	Mass recovery	pH		ORP		PCE (5 mg L^{-1})[a]	TCE (5 mg L^{-1})[a]	cDCE (5 mg L^{-1})[a]	1.1.1-TCA (5 mg L^{-1})[a]
	%	Initial	At the end	Initial	At the end	% reduced	% reduced	% reduced	% reduced
FeA4 (50 g L^{-1})	67	7.68	9.34	249	−113	97	100	42	100
FeH1 (50 g L^{-1})	93	7.18	11.00	260	−14	31	25	16	19
FeH3 (50 g L^{-1})	60	7.20	9.33	60	11	98	98	51	100
FeH4 (50 g L^{-1})	43	7.20	9.33	60	−289	100	98	98	100
FeH6 (50 g L^{-1})	68	7.20	10.24	60	−47	91	99	65	100
FeH7 (50 g L^{-1})	68	7.20	9.65	60	−152	96	99	42	100
FeH8 (50 g L^{-1})	54	7.20	10.09	60	−227	98	100	100	100
FeH9 (50 g L^{-1})	97	7.20	10.89	60	1	9	5	3	4
FeH10 (50 g L^{-1})	69	7.20	9.39	60	−94	88	51	30	46
FeH11 (50 g L^{-1})	29	7.20	10.55	60	−396	100*	100*	100*	100*
FeH12 (50 g L^{-1})	31	7.20	10.59	60	−272	100*	99*	87*	98*
FeH13 (50 g L^{-1})	66	7.18	10.02	260	−224	95	100	45	100
FeH14 (50 g L^{-1})	44	7.68	10.06	249	−294	100	100	99	100
FeQ2 (50 g L^{-1})	44	7.68	10.37	249	−314	100	100	100	100
MS200 (50 g L^{-1})	108	7.18	9.58	260	−27	69	8	1	100
MS200+ (50 g L^{-1})	75	7.18	9.74	260	−153	79	61	34	100
SM (50 g L^{-1})	83	7.18	9.15	260	−67	30	24	21	100
HQ (50 g L^{-1})	51	6.00	10.40	340	−140	99	100	88	100
Nanofer25s (5 g L^{-1})	11	7.87	8.45	39	−205	100	100	100	100
RNIP (5 g L^{-1})	32	7.87	10.91	39	−270	97	99	33	100
FeS Aldrich (50 g L^{-1})	65	7.68	6.48	249	−156	100	98	20	100
FeS BIO1 (40 g L^{-1})[b]	74	7.68	7.85	249	−299	37	26	16	62
FeS BIO2 (40 g L^{-1})[b]	91	7.68	7.95	249	−279	25	16	6	28

[a] Initial concentration or concentration range;
[b] Concentration calculated according to dry weight measurement and precipitation of organic matter.
* Sorption.

most reactive iron used in this study. A significantly high degradation capacity was also observed for the newly designed FeH14 iron.

In general, when comparing the reduction rates of the tested CAHs for the different irons (Table 4), 1,1,1-TCA is clearly degraded at the fastest rate (complete reduction was achieved within 14 days) by most of the studied irons. This might be explained by differences in bond strength between ethenes and ethanes (sp2 > sp3) [25]. cDCE was the least reactive examined pollutant as possible competition between cDCE and TCE can occur [39]. For the other pollutants, no fixed order of degradation was observed; it was dependent on the reaction mechanism [39–41] and in certain cases on the specific surface areas. Effect of iron surface area on the degradation kinetics was observed for irons produced from the same raw material (from FeH10 to FeH14). The iron with the lowest specific surface area (FeH10) had the slowest degradation rate of the examined chloroethenes, while the fastest degradation was observed for FeH14 iron (the highest specific surface area). A one-way analysis of variance (ANOVA) reported in SI4 revealed that lower ORP values were responsible for significant reduction of PCE, TCE and cDCE ($p < 0.01$). There was no correlation between k_{obs} and maximal observed pH values (SI5).

Furthermore, VC as an intermediate product did not increase significantly. Acetylene was detected in low concentrations indicating that the reductive-β-elimination pathway was followed with further degradation of acetylene to ethene and ethane. This is in accordance with previous studies [30,42]. In respect to iron sulfides, production of acetylene as an intermediate product was observed for both the commercial FeS and FeS BIO1, indicating on abiotic degradation of contaminants via the β-elimination pathway. This is consistent with conclusions from others research [14–16].

3.2. Mass normalized CAH-removal kinetics for different iron based particles

To obtain removal kinetic data that are independent of the mass of iron based particles, mass normalized degradation rate constants (k_M) were used (Table 3) and plotted for comparison in Fig. 1. Focusing on mZVI, FeH14 was found to be the most reactive microscale iron among all other newly produced mZVIs. FeH3 and FeH4, which are both different size fractions of the same metal powder, had a similar reactivity. This observation suggests there is no significant impact of particle size on iron efficiency in CAHs removal. A more detailed correlation analysis based on the data presented herein revealed that particle size and shape do not have a strong impact on observed mZVI reactivity (SI6 and SI7). This was also suggested for nZVIs by another research group [28]. Comparing the k_M values of the newly developed FeH14, FeH3 and FeH4 to the reactivity of the most reactive commercial microscale product (HQ), it is evidenced that these new irons have the similar or faster degradation rate for tested CAHs.

Calculated k_M values for PCE, TCE, cDCE and 1,1,1-TCA degradation by granular reference material (FeA4) and by mZVIs were similar. For Nanofer25s the k_M values were one to two orders of magnitude higher than the values for FeH14, FeH3, FeH4 and HQ. Nanofer25s is the most reactive among all studied iron based particles. FeS Aldrich gave k_M values for PCE, TCE and 1,1,1-TCA similar to the k_M values of highly reactive mZVIs and FeA4 iron, but was the least reactive towards cDCE among all examined irons (Fig. 1). After mass normalization, the reactivity of FeS BIO1 is one to two orders of magnitude lower than reference granular iron and similar to less reactive commercially available mZVIs (SM and MS200).

3.3. Surface area normalized kinetics for iron based materials

As reductive dehalogenation of CAHs by ZVI is a surface mediated process, the available ZVI surface is an important parameter. Several studies revealed that it is not just k_{obs} and k_M data that should be considered for examination of the zerovalent iron particles reactivity [24,25]. Also specific surface area normalized data (k_{SA}) can serve as general descriptor of iron reactivity [24,26], especially due to the higher reactive surface area of nanoscale particles (4–25 $m^2\,g^{-1}$) over microscale ones (0.1–4 $m^2\,g^{-1}$ for most of examined mZVIs). k_{SA} data for all iron particles tested in this work are presented in Table 3 and compared in Fig. 2.

Fig. 2 shows that differences in reactivity between iron particles are large (up to three orders of magnitude). The obtained k_{SA}

Table 3
Summary of kinetic data for dehalogenation of PCE, TCE, cDCE and 1,1,1-TCA by studied iron based particles.

Treatment (concentration)	PCE ($5\ mg\ L^{-1}$)[a] k_{ob} (h^{-1})[b]	PCE R^2 (n)[c]	PCE k_M ($L\ g^{-1}\ h^{-1}$)[d]	PCE k_{SA} ($L\ m^{-2}\ h^{-1}$)[e]	TCE ($5\ mg\ L^{-1}$)[a] k_{ob} (h^{-1})[b]	TCE R^2 (n)[c]	TCE k_M ($L\ g^{-1}\ h^{-1}$)[d]	TCE k_{SA} ($L\ m^{-2}\ h^{-1}$)[e]
FeA4 ($50\ g\ L^{-1}$)	1.6E−03	0.78 (5)	3.2E−05	2.8E−05	2.4E−03	0.83 (5)	4.9E−05	4.2E−05
FeH1 ($50\ g\ L^{-1}$)	3.9E−04	0.99 (3)	7.8E−06	2.9E−05	3.8E−04	0.99 (3)	7.6E−06	2.8E−05
FeH3 ($50\ g\ L^{-1}$)	1.5E−03	0.98 (5)	3.1E−05	4.9E−04	2.8E−03	0.96 (4)	5.6E−05	8.8E−04
FeH4 ($50\ g\ L^{-1}$)	1.7E−03	0.97 (3)	3.5E−05	3.7E−04	3.1E−03	0.98 (4)	6.1E−05	6.5E−04
FeH6 ($50\ g\ L^{-1}$)	9.0E−04	0.97 (5)	1.8E−05	2.0E−04	2.9E−03	0.99 (4)	5.7E−05	6.4E−04
FeH7 ($50\ g\ L^{-1}$)	1.3E−03	0.99 (5)	2.6E−05	2.1E−04	3.9E−03	0.91 (4)	7.7E−05	6.2E−04
FeH8 ($50\ g\ L^{-1}$)	1.3E−03	0.92 (5)	2.7E−05	7.7E−05	2.2E−03	0.97 (4)	4.4E−05	1.3E−04
FeH9 ($50\ g\ L^{-1}$)	9.6E−05	0.87 (3)	1.9E−06	3.8E−06	4.2E−05	0.98 (3)	8.3E−07	1.7E−06
FeH10 ($50\ g\ L^{-1}$)	3.2E−03[f]	0.68 (3)	6.3E−05	5.2E−05	7.0E−04	0.71 (3)	1.4E−05	1.1E−05
FeH11 ($50\ g\ L^{-1}$)	2.0E−02	1.00 (2)	3.9E−04	9.9E−05	1.2E−02	1.00 (2)	2.4E−04	5.9E−05
FeH12 ($50\ g\ L^{-1}$)	1.9E−02	1.00 (2)	3.7E−04	1.0E−04	1.1E−02	1.00 (2)	2.1E−04	5.9E−05
FeH13 ($50\ g\ L^{-1}$)	3.8E−03	1.00 (2)	7.6E−05	5.1E−05	7.1E−03	1.00 (2)	1.4E−04	9.5E−05
FeH14 ($50\ g\ L^{-1}$)	2.3E−02	1.00 (2)	4.7E−04	4.1E−05	9.8E−03	0.80 (3)	2.0E−04	1.7E−05
FeQ2 ($50\ g\ L^{-1}$)	2.1E−03	0.92 (3)	4.1E−05	1.0E−04	4.5E−03	0.97 (4)	9.1E−05	2.3E−04
MS200 ($50\ g\ L^{-1}$)	4.9E−04	0.62 (5)	9.8E−06	2.7E−05	4.1E−04	0.98 (5)	8.3E−06	2.3E−05
MS200+ ($50\ g\ L^{-1}$)	4.9E−04	0.62 (5)	9.8E−06	2.1E−05	3.8E−04	0.79 (5)	7.7E−06	1.6E−05
SM ($50\ g\ L^{-1}$)	1.3E−04	0.94 (5)	2.5E−06	5.2E−06	1.0E−04	0.99 (5)	2.1E−06	4.3E−06
HQ ($50\ g\ L^{-1}$)	7.0E−03	0.99 (3)	1.4E−04	1.7E−04	3.3E−03	0.99 (3)	6.7E−05	8.2E−05
Nanofer25s ($5\ g\ L^{-1}$)	1.4E−02	0.97 (4)	2.7E−03	1.1E−04	1.2E−02	0.91 (5)	2.5E−03	9.8E−05
RNIP ($5\ g\ L^{-1}$)	7.1E−03	0.92 (5)	1.3E−03	2.6E−04	9.6E−03	0.81 (5)	1.8E−03	3.5E−04
FeS Aldrich ($50\ g\ L^{-1}$)	4.2E−03	1.00 (4)	8.4E−05	9.3E−05	6.6E−03	0.85 (3)	1.3E−04	1.5E−04
FeS BIO1 ($40\ g\ L^{-1}$)	6.4E−04	0.76 (3)	1.7E−05	4.9E−06	4.2E−04	0.74 (3)	1.1E−05	3.2E−06
FeS BIO2 ($40\ g\ L^{-1}$)	1.4E−04	0.73 (5)	3.8E−06	1.1E−06	1.3E−04	0.99 (4)	3.4E−06	1.0E−06

Treatment (concentration)	cDCE ($5\ mg\ L^{-1}$)[a] k_{ob} (h^{-1})[b]	cDCE R^2 (n)[c]	cDCE k_M ($L\ g^{-1}\ h^{-1}$)[d]	cDCE k_{SA} ($L\ m^{-2}\ h^{-1}$)[e]	1,1,1-TCA ($5\ mg\ L^{-1}$)[a] k_{ob} (h^{-1})[b]	1,1,1-TCA R^2 (n)[c]	1,1,1-TCA k_M ($L\ g^{-1}\ h^{-1}$)[d]	1,1,1-TCA k_{SA} ($L\ m^{-2}\ h^{-1}$)[e]
FeA4 ($50\ g\ L^{-1}$)	2.0E−04	0.91 (5)	3.9E−06	3.4E−06	1.9E−02	1.00 (2)	3.9E−04	3.4E−04
FeH1 ($50\ g\ L^{-1}$)	2.6E−04	1.00 (3)	5.3E−06	1.9E−05	2.7E−04	0.99 (3)	5.3E−06	2.0E−05
FeH3 ($50\ g\ L^{-1}$)	2.5E−04	0.90 (5)	5.1E−06	8.1E−05	4.4E−03	0.99 (4)	8.7E−05	1.4E−03
FeH4 ($50\ g\ L^{-1}$)	1.2E−03	0.79 (5)	2.4E−05	2.6E−04	6.2E−03	1.00 (2)	1.2E−04	1.3E−03
FeH6 ($50\ g\ L^{-1}$)	3.6E−04	0.87 (5)	7.3E−06	8.2E−05	6.3E−03	0.96 (3)	1.3E−04	1.4E−03
FeH7 ($50\ g\ L^{-1}$)	1.9E−04	0.90 (5)	3.8E−06	3.1E−05	5.9E−03	0.99 (3)	1.2E−04	9.4E−04
FeH8 ($50\ g\ L^{-1}$)	8.0E−04	0.98 (4)	1.6E−05	4.6E−05	1.6E−02	1.00 (2)	3.2E−04	9.2E−04
FeH9 ($50\ g\ L^{-1}$)	3.3E−05	0.57(3)	6.7E−07	1.3E−06	3.3E−05	0.84 (3)	6.7E−07	1.3E−06
FeH10 ($50\ g\ L^{-1}$)	1.3E−04	0.93 (5)	2.6E−06	2.1E−06	2.5E−04	0.75 (5)	5.0E−06	4.1E−06
FeH11 ($50\ g\ L^{-1}$)	3.6E−03	1.00 (2)	7.3E−05	1.8E−05	8.8E−03	1.00 (2)	1.8E−04	4.4E−05
FeH12 ($50\ g\ L^{-1}$)	3.0E−03	1.00 (2)	6.1E−05	1.7E−05	7.8E−03	1.00 (2)	1.6E−04	4.3E−05
FeH13 ($50\ g\ L^{-1}$)	2.0E−04	0.80 (5)	3.9E−06	2.6E−06	1.8E−02	1.00 (2)	3.5E−04	2.3E−04
FeH14 ($50\ g\ L^{-1}$)	2.1E−03	0.81 (5)	4.1E−05	3.6E−06	2.0E−02	1.00 (2)	4.0E−04	3.5E−05
FeQ2 ($50\ g\ L^{-1}$)	1.4E−03	0.87 (3)	2.8E−05	6.9E−05	2.5E−02	1.00 (2)	5.1E−04	1.3E−03
MS200 ($50\ g\ L^{-1}$)	6.3E−05	0.98 (5)	1.3E−06	3.5E−06	1.3E−02	1.00 (2)	2.6E−04	7.3E−04
MS200+ ($50\ g\ L^{-1}$)	1.8E−04	0.52 (5)	3.6E−06	7.6E−06	2.5E−02	1.00 (2)	5.1E−04	1.1E−03
SM ($50\ g\ L^{-1}$)	9.2E−05	0.93 (5)	1.8E−06	3.8E−06	4.0E−03	0.88 (3)	8.0E−05	1.7E−04
HQ ($50\ g\ L^{-1}$)	9.8E−04	0.82 (5)	1.9E−05	2.4E−05	2.5E−02	1.00 (2)	4.9E−04	6.0E−04
Nanofer25s ($5\ g\ L^{-1}$)	1.0E−02	0.99 (4)	2.0E−03	8.2E−05	1.2E−01	1.00 (2)	2.3E−02	9.4E−04
RNIP ($5\ g\ L^{-1}$)	8.8E−04	0.62 (5)	1.6E−04	3.2E−05	1.5E−02	0.99 (4)	2.8E−03	5.6E−04
FeS Aldrich ($50\ g\ L^{-1}$)	5.8E−05	0.46 (5)	1.2E−06	1.3E−06	2.5E−02	1.00 (2)	5.0E−04	5.5E−04
FeS BIO1 ($40\ g\ L^{-1}$)	2.9E−04	0.75 (3)	7.5E−06	2.2E−06	4.3E−04	0.80(5)	1.1E−05	3.2E−06
FeS BIO2 ($40\ g\ L^{-1}$)	1.8E−04	0.98 (3)	4.8E−06	1.4E−06	1.5E−04	0.88(5)	4.0E−06	1.2E−06

[a] Initial concentration or concentration range;
[b] k_{ob} the first order decay constant (h^{-1});
[c] n, number of data points included in fitting the disappearance kinetic;
[d] k_M the mass normalized first order decay constant ($L\ g^{-1}\ h^{-1}$);
[e] k_{SA} surface area normalized reaction rate constants ($L\ m^{-2}\ h^{-1}$);
[f] Underlined data present sorption rate constants.

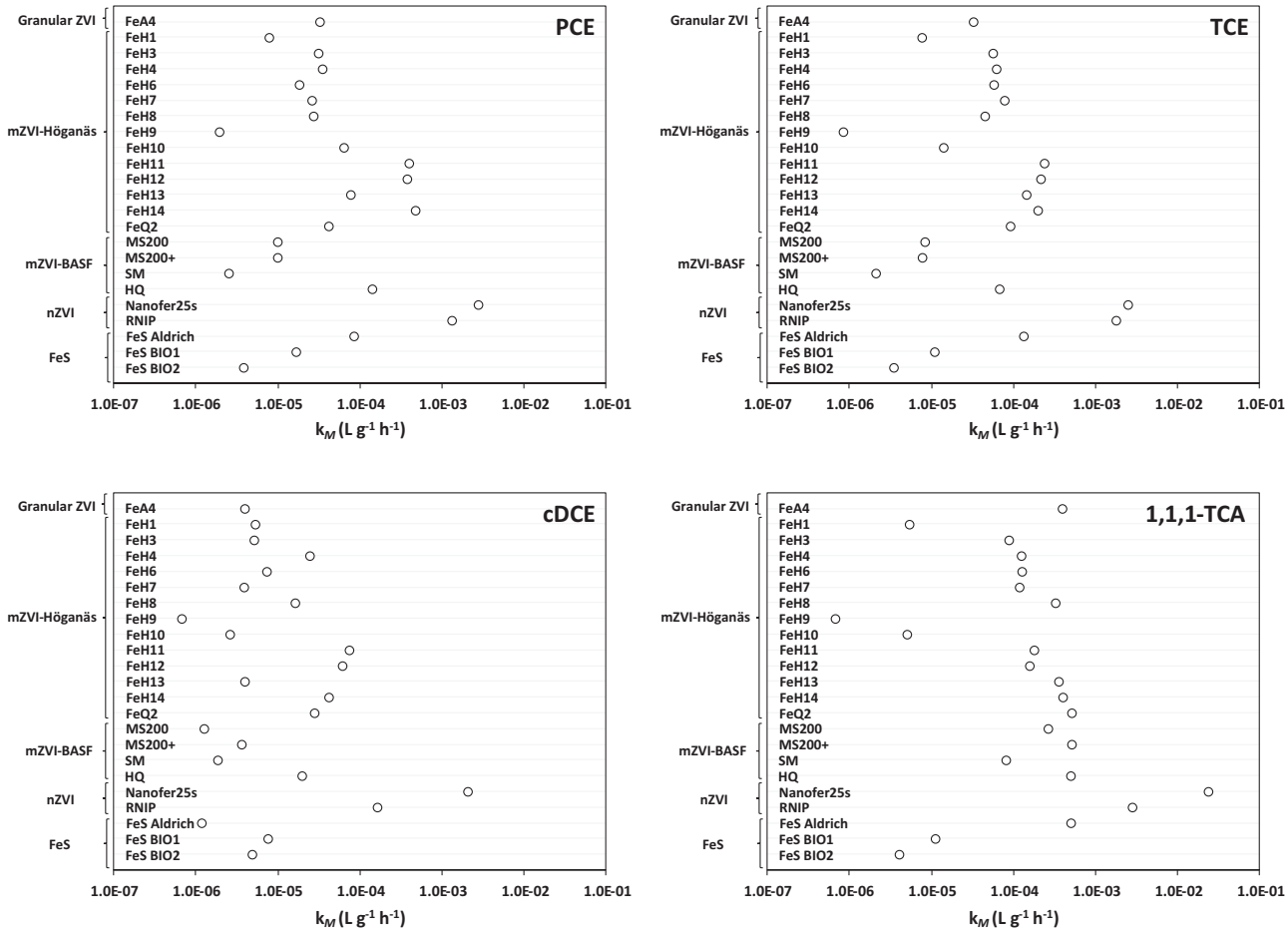

Fig. 1. Distribution of mass normalized rate constants for the reduction of PCE, TCE, cDCE and 1,1,1-TCA by different zerovalent iron particles and iron sulfides. Quantitative results are summarized in Table 3.

values for all tested mZVIs are similar or one to two orders of magnitude different than representative average literature k_{SA} values of $2.1 \pm 2.7 \times 10^{-3}$ L m $^{-2}$ h^{-1} (PCE), $3.9 \pm 3.6 \times 10^{-4}$ L m $^{-2}$ h^{-1} (TCE), $4.1 \pm 1.7 \times 10^{-5}$ L m $^{-2}$ h^{-1} (cDCE) and 1.1×10^{-2} L m $^{-2}$ h^{-1} (1,1,1-TCA) for commercial iron particles [24]. Based on k_{SA} data, FeH3 and FeH4 were the most reactive towards CAHs among other mZVIs. Interestingly, k_{SA} (PCE, TCE and cDCE) obtained with FeH3 and FeH4 were approximately 1 to 5 times higher than for Nanofer25s. The rate constants obtained for the granular reference material (FeA4) and commercially available mZVIs are in the same order of magnitude. The distribution of k_{SA} values shows that the reactivity of the commercially available FeS (Aldrich) and granular ZVI are in the same order of magnitude. Moreover, the k_{SA} values for biogenic iron sulfides are similar to the k_{SA} values of the least reactive mZVIs. This implies that biogenic iron sulfides are not highly reactive, but can contribute to slow reduction of CAHs in natural systems.

Finally, data in Fig. 2 suggest that some newly designed microscale zerovalent iron particles, and especially FeH4, can be considered as promising particles for remediation of the studied CAHs. FeH4 was capable of removal of all pollutants, as well as slow degradation of intermediate product 1,1-dichloroethane (1,1-DCA) as shown in Fig. 3.

Table 4
Comparison of the PCE, TCE, cDCE and 1,1,1-TCA reduction rates for each iron based particles.

Order of reduction rates	Iron based particle
1,1,1-TCA > TCE > PCE > cDCE	FeA4; RNIP; FeH3; FeH4; FeH6; FeH7; FeH8; FeH13; FeQ2; HQ
1,1,1-TCA > PCE > TCE > cDCE	FeS Aldrich; MS200; SM; MS 200+; Nanofer25s
PCE > TCE > 1,1,1-TCA > cDCE	FeH1; FeH10; FeH11; FeH12; FeH14
cDCE > PCE > 1,1,1-TCA > TCE	FeH9
PCE ≥ 1,1,1-TCA > TCE > cDCE	FeS BIO1, FeS BIO2

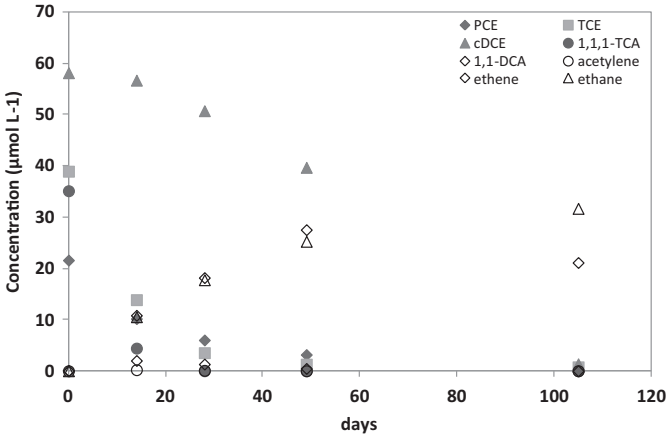

Fig. 3. Reduction of different CAHs by 50 g L^{-1} of FeH4 iron.

3.4. 1,1-DCA

1,1-DCA is a degradation product of 1,1,1-TCA that has been reported to be degradable by ZVI [33,43]. Degradation of this pollutant, however, is slow and a laboratory abiotic degradation half-life

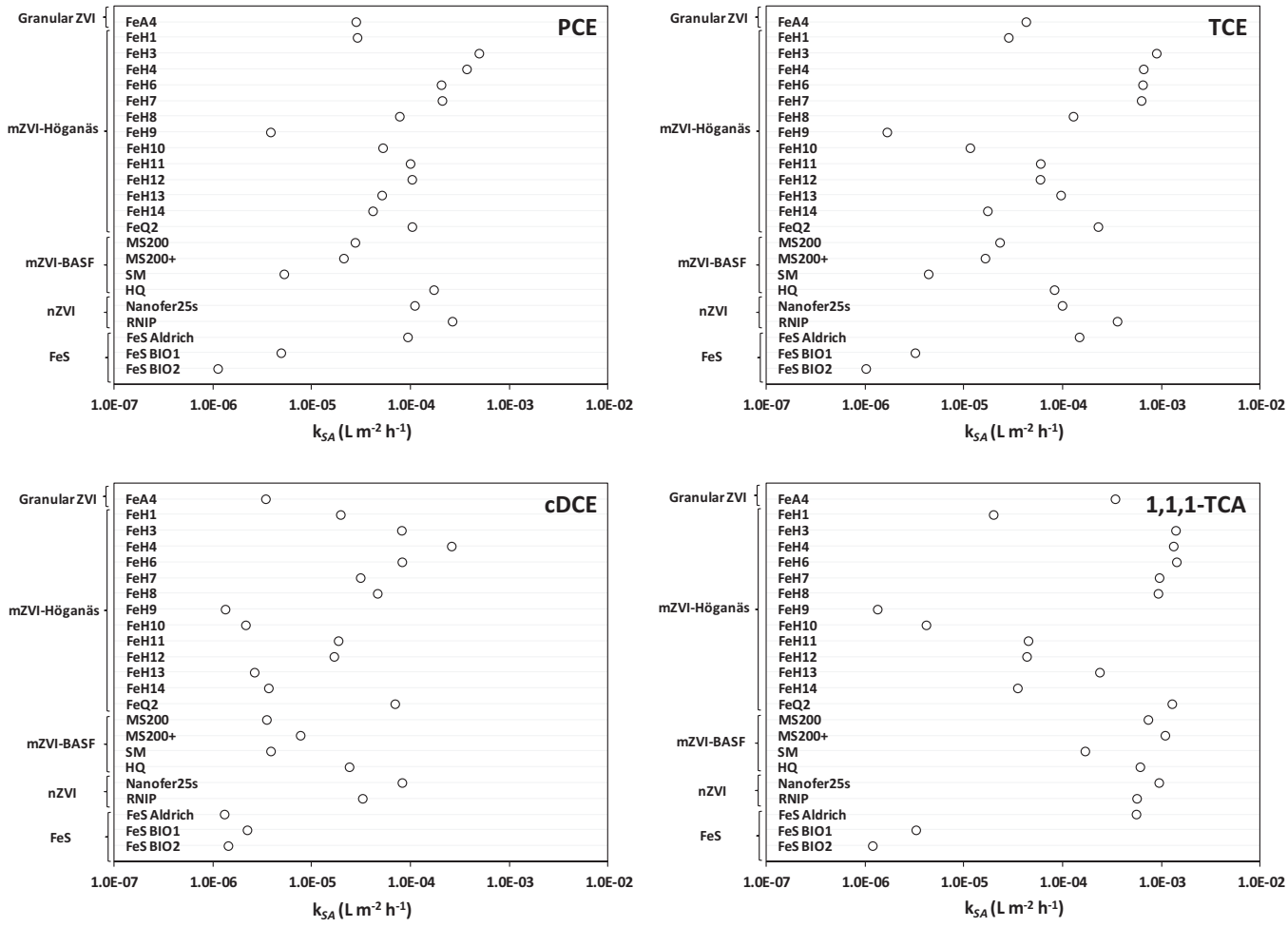

Fig. 2. Distribution of surface area normalized rate constants for the reduction of PCE, TCE, cDCE and 1,1,1-TCA by different iron particles and iron sulfides. Quantitative results are summarized in Table 3.

Table 5
1,1-DCA appearance with degradation rates for studied iron based particles (values reported as a mean of triplicates) in the batch reactors.

	1,1-DCA		
Treatment	(% produced) [a]	k_{ob} (h^{-1})[b]	R^2 (n)[c]
FeA4 (50 g L^{-1})	40.7	7.5×10^{-5}	1.00 (2)
FeH1 (50 g L^{-1})	0.37	*	*
FeH3 (50 g L^{-1})	5.90	4.3×10^{-4}	0.99 (3)
FeH4 (50 g L^{-1})	5.71	2.4×10^{-3}	0.81 (3)
FeH6 (50 g L^{-1})	9.27	2.2×10^{-4}	0.96 (3)
FeH7 (50 g L^{-1})	8.73	2.7×10^{-4}	0.93 (3)
FeH8 (50 g L^{-1})	25.1	2.5×10^{-4}	0.93 (3)
FeH9 (50 g L^{-1})	0.19	*	*
FeH10 (50 g L^{-1})	1.87	*	*
FeH11 (50 g L^{-1})	1.38	*	*
FeH12 (50 g L^{-1})	2.26	*	*
FeH13 (50 g L^{-1})	26.9	2.2×10^{-4}	1.00 (2)
FeH14 (50 g L^{-1})	4.00	5.7×10^{-4}	0.98 (4)
FeQ2 (50 g L^{-1})	25.9	3.4×10^{-4}	0.87 (4)
MS200 (50 g L^{-1})	65.8	*	*
MS200+ (50 g L^{-1})	65.2	8.8×10^{-4}	0.99 (4)
SM (50 g L^{-1})	20.0	2.0×10^{-4}	1.00 (2)
HQ (50 g L^{-1})	42.4	2.3×10^{-4}	0.91 (4)
Nanofer25s (5 g L^{-1})	18.6	1.2×10^{-3}	0.99 (4)
RNIP (5 g L^{-1})	6.29	*	*
FeS Aldrich (50 g L^{-1})	26.1	4.0×10^{-4}	0.08 (4)
FeS BIO1 (40 g L^{-1})	3.25	*	*
FeS BIO2 (40 g L^{-1})	3.11	*	*

[a] 1,1-DCA production as an intermediate product in 1,1,1-TCA degradation–expressed as maximal observed percentage of total 1,1,1-TCA;
[b] k_{ob} the pseudo-first-order decay constant (h^{-1});
[c] *n*, number of data points;
* No degradation observed.

of 61 years has been reported [44]. In this study, increased 1,1-DCA concentrations were observed for most tested iron based particles, but the maximal observed amount of 1,1-DCA produced during 1,1,1-TCA degradation was found to depend on the particles type (Table 5). The most pronounced production of 1,1-DCA was observed for FeA4, MS200, MS200+ and HQ (40–65%), while the lowest levels were measured for FeH1 and FeH9 (<0.4%). In respect to 1,1-DCA degradation, the fastest degradation rates $2.4 \times 10^{-3}\ h^{-1}$ and $1.2 \times 10^{-3}\ h^{-1}$ were observed for FeH4 and Nanofer25s respectively.

An additional batch degradation experiment with 1,1,1-TCA as single pollutant was performed using FeH4 to examine 1,1,1-TCA degradation and 1,1-DCA formation/degradation more in detail (SI8). Approximately 70% of the 1,1,1-TCA was found to be transformed to acetic acid by hydrolysis. The 1,1,1-TCA hydrolysis pathway has been reported before [45]. The remaining 28 percent obtained herein were transformed to ethane, while only 2 percent were transformed to 1,1-DCA by reductive dechlorination. The pronounced production of 1,1-DCA observed for several irons involved the α-elimination and hydrogenolysis pathway in degradation of 1,1,1-TCA. Chemical transformation of 1,1,1-TCA by these pathways has also been reported previously [33].

4. Conclusions

Reactivity data were collected for 23 reactive iron based particles via standardized test procedure allowing reactivity comparison

between the different materials towards different pollutants within a reasonable amount of time. The reactivity of the particles was compared based on k_{obs} and k_M data, as well as k_{SA} values. As an appropriate descriptor of the overall surface reactivity of the particles and contaminants degradation kinetics, k_{SA} data were used for the selection of the most promising iron for in situ application.

The obtained k_{SA} values show that the microscale iron particles FeH3 and FeH4 perform mostly better than Nanofer25s and commercially available mZVIs. The k_{SA} values of commercial FeS were similar to that of the granular ZVI material selected as a reference material. The reactivity of commercial FeS and granular ZVI towards 1,1,1-TCA was in the same order of magnitude as Nanofer25s and some mZVIs. On the other hand, their PCE, TCE and cDCE degradation kinetics were one to two orders of magnitude slower than Nanofer25s and some mZVIs. This study also suggests that biogenic iron sulfides may contribute to the reductive degradation of mainly 1,1,1-TCA, although they were the least reactive among all studied irons. No correlation was found between reactivity of the examined particles and particle size or pH. Except for pH increase to approximately 11 where particles were found non-reactive. In general, significantly reduced ORP values were found good indicators for reactive particles. The impact of the particle composition on its reactivity is under investigation (manuscript being submitted).

The large data set resulting from this study, shows that some of the newly designed mZVI particles introduced in this study have promising reactive properties for in situ remediation applications, also towards 1,1-DCA. These particles are relatively low-cost and easy to handle compared to nZVIs.

Acknowledgments

This research was conducted in the framework of the European Union project AQUAREHAB (FP7 - Grant Agreement Nr. 226565). We thank the support of Prof. Dr. Piet Seuntjens. We would also like to thank Prof. Dr. Rajandrea Sethi for his appreciated contribution to this study.

Appendix A. Supplementary data

Supplementary data associated with this article can be found, in the online version, at http://dx.doi.org/10.1016/j.jhazmat.2013.02.047.

References

[1] R.W. Gillham, S.F. O'Hannesin, Enhanced degradation of halogenated aliphatics by zerovalent iron, Ground Water. 32 (1994) 958–971.
[2] A.R. Gavaskar, Design and construction techniques for permeable reactive barriers, J. Hazard. Mater. 68 (1999) 41–71.
[3] P.G. Tratnyek, T.L. Johnson, M.M. Scherer, G.R. Eykholt, Remediating groundwater with zero-valent metals: Kinetic considerations in barrier design, Ground Water Monit. Remediation 17 (1997) 108–114.
[4] K.C.K. Lai, I.M.C. Lo, P. Kjeldsen, Remediation of Chlorinated Aliphatic Hydrocarbons in Groundwater using Fe^0 PRB, in: G.A. Boshoff, B.D. Bone (Eds.), Permeable Reactive Barriers, IAHS press, Wallingford, 2005, pp. 12–22.
[5] C. Noubactep, S. Caré, On nanoscale metallic iron for groundwater remediation, J. Hazard. Mater. 182 (2010) 923–927.
[6] C. Noubactep, S. Caré, R.A. Crane, Nanoscale metallic iron for environmental remediation: prospects and limitations, Water Air Soil Pollut. 223 (2012) 1363–1382.
[7] T. Phenrat, N. Saleh, R.D. Tilton, G.V. Lowry, Aggregation, Sedimentation of Aqueous Nanoscale Zerovalent Iron Dispersions, Environ. Sci. Technol. 41 (2007) 284–290.
[8] C. Lee, J.Y. Kim, W.I. Lee, K.L. Nelson, J. Yoon, D.L. Sedlak, Bactericidal effect of zerovalent iron nanoparticles on Escherichia coli, Environ. Sci. Technol. 42 (2008) 4927–4933.
[9] H. Li, Q. Zhou, Y. Wu, J. Fu, T. Wang, G. Jiang, Effects of waterborne nano-iron on medaka (*Oryzias latipes*): antioxidant enzymatic activity, lipid peroxidation and histopathology, Ecotoxicol. Environ. Saf. 72 (2009) 684–692.
[10] T. Phenrat, Y. Liu, R.D. Tilton, G.V. Lowry, Adsorbed polyelectrolyte coatings decrease Fe^0 nanoparticle reactivity with TCE in water: conceptual model and mechanisms, Environ. Sci. Technol. 43 (2009) 1507–1514.
[11] E.C. Butler, K.F. Hayes, Kinetics of the transformation of halogenated aliphatic compounds by iron sulfide, Environ. Sci. Technol. 34 (2000) 422–429.
[12] E.C. Butler, K.F. Hayes, Factors influencing rates and products in the transformation of trichloroethylene by iron sulfide and iron metal, Environ. Sci. Technol. 35 (2001) 3884–3891.
[13] J.W. Gander, G.F. Parkin, M.M. Scherer, Kinetics of 1,1,1-trichloroethane transformation by iron sulfide and 1 methanogenic consortium, Environ, Sci. Technol. 36 (2002) 4540–4546.
[14] H.Y. Jeong, H. Kim, K.F. Hayes, Reductive Dechlorination Pathways of Tetrachloroethylene and Trichloroethylene and Their Products by Mackinawite (FeS) in the Presence of Metals, Environ. Sci. Technol. 41 (2007) 7736–7743.
[15] Y.T. He, J.T. Wilson, R. Wilkin, Impact of iron sulfide transformation on trichloroethylene degradation, Geochim. Cosmochim. Acta 74 (2010) 2025–2039.
[16] W. Zhang, C.B. Wang, H.L. Lien, Treatment of chlorinated organic contaminants with nanoscale bimetallic particles, Catal. Today 40 (1998) 387–395.
[17] Y. Xu, W. Zhang, Subcolloidal Fe/Ag particles for reductive dehalogenation of chlorinated benzenes, Ind. Eng. Chem. Res. 39 (2000) 2238–2244.
[18] B. Schrick, J.L. Blough, A.D. Jones, T.E. Mallouk, Hydrodechlorination of trichloroethylene to hydrocarbons using bimetallic nickel–iron nano-scale particles, Chem. Mater. 14 (2002) 5140–5147.
[19] R.J. Barnes, O. Riba, M.N. Gardner, T.B. Scott, S.A. Jackman, I.P. Thompson, Optimization of nano-scale nickel/iron particles for the reduction of high concentration chlorinated aliphatic hydrocarbon solutions, Chemosphere 79 (2010) 448–454.
[20] W. Zhang, Nanoscale iron particles for environmental remediation: An overview, J. Nanopart. Res. 5 (2003) 323–332.
[21] J. Nurmi, P. Tratnyek, V. Sarathy, D. Baer, J. Amonette, K. Pecher, C. Wang, J. Linehan, D. Watson, R. Penn, M. Driessen, Characterization and properties of Metallic Iron Nanoparticles: Spectroscopy, Electrochemistry and Kinetics, Environ. Sci. Technol. 39 (2005) 1221–1230.
[22] C. Mace, Controlling groundwater VOCs: do nanoscale ZVI particles have any advantages over microscale ZVI or BNP, Pollut. Eng. 38 (2006) 24–27.
[23] S. Comba, A. Di Molfetta, R.A. Sethi, Comparison Between Field Applications of Nano-, Micro-, and Millimetric Zero-Valent Iron for the Remediation of Contaminated Aquifers, Water Air Soil Pollut. 215 (2011) 595–607.
[24] T.L. Johnson, M.M. Scherer, P.G. Tratnyek, Kinetics of halogenated organic compound degradation by iron metal, Environ. Sci. Technol. 30 (1996) 2634–2640.
[25] M.M. Scherer, B.A. Balko, D.A. Gallagher, P.G. Tratnyek, Correlation analysis of rate constants for dechlorination by zero-valent iron, Environ. Sci. Technol. 32 (1998) 3026–3033.
[26] R. Miehr, P.G. Tratnyek, J.Z. Bandstra, M.M. Scherer, M.J. Alowitz, E.J. Bylaska, Diversity of contaminant reduction reactions by zerovalent iron: Role of the reductate, Environ. Sci. Technol. 38 (2004) 139–147.
[27] J. Hara, H. Ito, K. Suto, C. Inoue, T. Chida, Kinetics of trichloroethene dechlorination with iron powder, Water Res. 39 (2005) 1165–1173.
[28] Y.Q. Liu, S.A. Majetich, R.D. Tilton, D.S. Sholl, G.V. Lowry, TCE dechlorination rates, pathways, and efficiency of nanoscale iron particles with different properties, Environ, Sci. Technol. 39 (2005) 1338–1345.
[29] C. Ma, Y. Wu, Dechlorination of perchloroethylene using zerovalent metal and microbial community, Environ. Geol. 55 (2008) 47–54.
[30] J. Farrell, M. Kason, N. Melitas, T. Li, Investigation of the long-term performance of zero-valent iron for reductive dechlorination of trichloroethylene, Environ. Sci. Technol. 34 (2000) 514–521.
[31] P. Bayer, M. Finkel, Modeling of sequential groundwater treatment with zerovalent iron and granular activated carbon, J. Contam. Hydrol. 78 (2005) 129–146.
[32] S.F. Cheng, S.C. Wu, The enhancement methods for the degradation of TCE by zero-valent metals, Chemosphere 41 (2000) 1263–1270.
[33] H. Song, E.R. Carraway, Reduction of chlorinated ethanes by nanosized zerovalent iron: Kinetics, pathways, and effects of reaction conditions, Environ. Sci. Technol. 39 (2005) 6237–6245.
[34] Y. Cho, S.I. Choi, Degradation of PCE, TCE and 1,1,1-TCA by nanosized FePd bimetallic particles under various experimental conditions, Chemosphere 81 (2010) 940–945.
[35] J. Dries, L. Bastiaens, D. Springael, S.N. Agathos, L. Diels, Combined removal of chlorinated ethenes and heavy metals by zerovalent iron in batch and continuous flow column systems, Environ. Sci. Technol. 39 (2005) 8460–8465.
[36] J.R. Postgate, The J'ulphate-Reducing Bacteria, Cambridge University Press, Cambridge, 1984.
[37] D.R. Burris, C.A. Delcomyn, M.H. Smith, A.L. Roberts, Reductive dechlorination of tetrachloroethylene and trichloroethylene catalyzed by Vitamin B12 in homogeneous and heterogeneous systems, Environ. Sci. Technol. 30 (1999) 3047–3052.
[38] C. Su, R.W. Puls, Kinetics of trichloroethene reduction by zerovalent iron and tin: pretreatment effect, apparent activation energy, and intermediate products, Environ. Sci. Technol. 33 (1999) 163–168.
[39] D. Schafer, R. Kober, A. Dahmke, Competing, TCE and cis-DCE degradation kinetics by zero-valent iron-experimental results and numerical simulation, J. Contam. Hydrol. 65 (2003) 183–202.
[40] M. Ebert, R. Kober, A. Parbs, V. Plagentz, D. Schafer, A. Dahmke, Assessing degradation rates of chlorinated ethylenes in column experiments with commercial iron materials used in permeable reactive barriers, Environ. Sci. Technol. 40 (2006) 2004–2010.
[41] W.A. Arnold, A.L. Roberts, Inter- and intraspecies competitive effects in reactions of chlorinated ethylenes with zero-valent iron in column reactors, Environ. Eng. Sci. 17 (2000) 291–302.

[42] A.L. Roberts, L.A. Totten, W.A. Arnold, D.R. Burris, T.J. Campbell, Reductive elimination of chlorinated ethylenes by zero-valent metals, Environ. Sci. Technol. 30 (1996) 2654–2659.
[43] R. Lookman, L. Bastiaens, B. Borremans, M. Maesen, J. Gemoets, L. Diels, Batch-test study on the dechlorination of 1,1,1-trichloroethane in contaminated aquifer material by zero-valent iron, J, Contam. Hydrol. 74 (2004) 133–144.
[44] P.M. Jeffers, L.M. Ward, L.M. Woytowitch, N.L. Wolfe, Homogeneous hydrolysis rate constants for selected chlorinated methanes, ethanes, ethenes, and propanes, Environ, Sci. Technol. 23 (1989) 965–969.
[45] P.L. McCarty, Biotic and Abiotic Transformations of Chlorinated Solvents in Groundwater, In Proceedings of the Symposium on Natural Attenuation of Chlorinated Organics in Groundwater, United States Environmental Protection Agency, Washington D.C., EPA/540/R-97/504, 1997 pp. 7-11.

Supporting Information.

Reactivity Screening of Microscale Zerovalent Irons and Iron Sulfides towards Different CAHs under Standardized Experimental Conditions

Milica Velimirovic,[a,b] Per-Olof Larsson,[c] Queenie Simons,[a] Leen Bastiaens[a,*]

[a]Flemish Institute for Technological Research (VITO), Boeretang 200, 2400, Mol, Belgium;

[b]University of Antwerp, Department of Bio-Engineering, Groenenborgerlaan 171, 2020 Antwerp, Belgium;

[c]Höganäs AB, Global Development, Bruksgatan 35, 26383 Sweden.

SI1. PCE, TCE, cDCE and 1,1,1-TCA reaction rate constants for different iron based particles. Lines present pseudo-first-order fit of data.

SI2. Calculation approach used for determination of k_{obs}.

SI3. Change of pH and ORP values in time (days).

SI4. Correlation between minimal observed ORP-values and PCE, TCE, cDCE and 1,1,1-TCA disappearance rate constants. In predicting the cDCE values data from Nanofer 25s were excluded as one anomalous point.

SI5. Correlation between maximal observed pH-values and PCE, TCE, cDCE and 1,1,1-TCA disappearance rate constants.

SI6. SEM images of several investigated microscale iron powders: (a) FeH4; (b) FeH7; (c) FeH8; (d) FeH12, (e) FeH13 and (f) BASF MS200.

SI7. Correlation between k_{obs} (h^{-1}) and iron particle size distribution D_{90} (μm) for all tested reactive materials.

SI8. Reduction of 1,1,1-TCA by 50 g L^{-1} of FeH4 iron. Symbols are average concentrations from triplicate reactors.

SI1. PCE, TCE, cDCE and 1,1,1-TCA reaction rate constants for different iron based particles. Lines present pseudo-first-order fit of data.

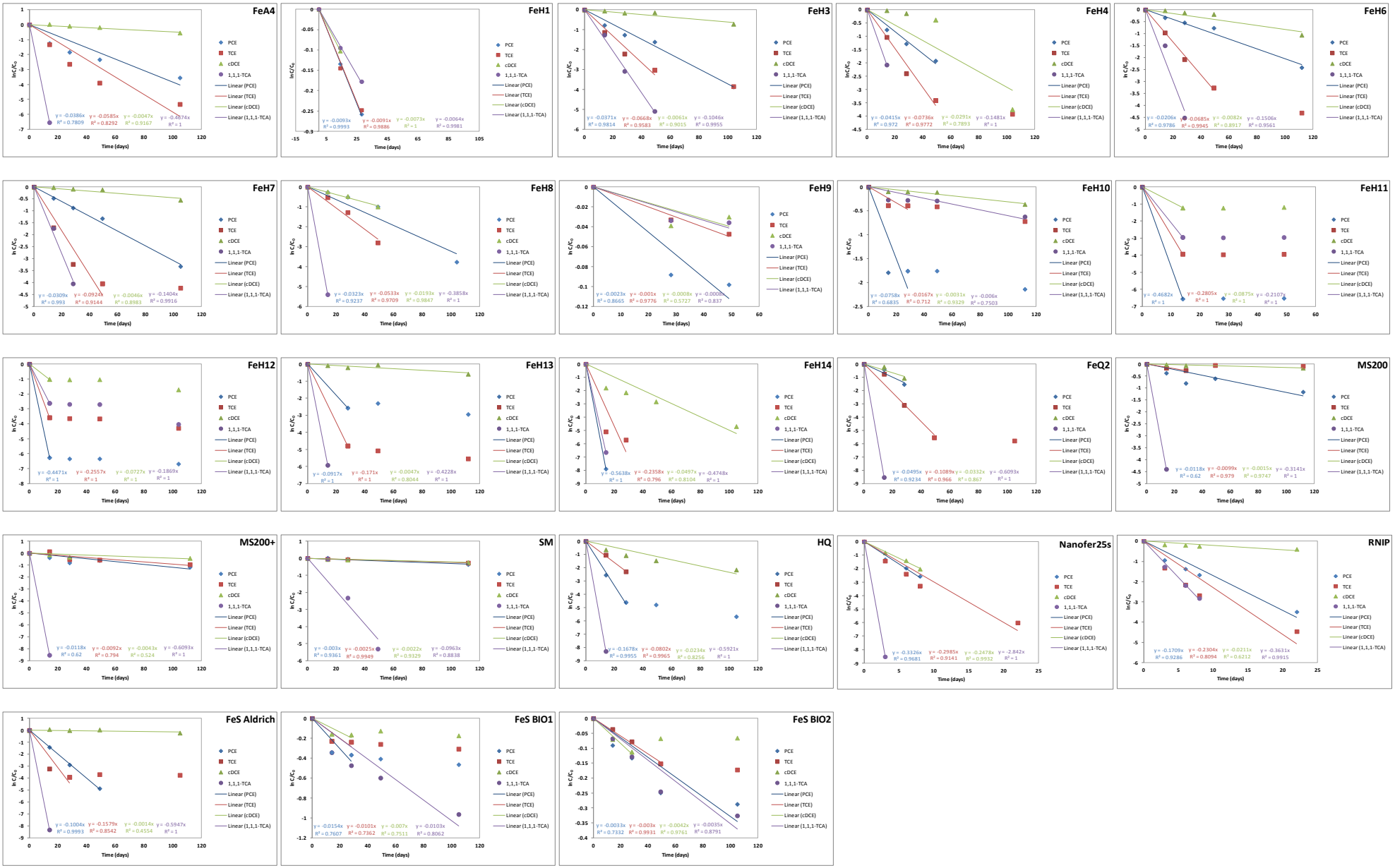

SI2. Calculation approach used for determination of k_{obs}.

k_{obs} was determined via linear regression of ln-transformed data (Eq. 2). The slope of the degradation rate curves (see SI1) represents k_{obs}. This is a commonly used approach to determine first order degradation rate constants, where it is known that low concentration data may have overestimated impact on the result. Generally, all measured data points were used to determine the curves. However, low concentration data were omitted when already proceeding by low concentration data (e.g. FeH3, FeH4, FeH6). For a number of iron particles the CAH-concentration decrease stopped after the second data point, indicating the sorption effects were dominant. In these cases, the sorption rates were calculated. For irons with a mixed removal mechanisms (degradation and sorption), the first order degradation rates were calculated and the lower correlation coefficient indicated the mixed effect.

More in detail, most of the examined iron based materials reduced 1,1,1-TCA rapidly, and gave first-order disappearance rate for PCE, TCE and cDCE. However, five of all tested mZVI materials (FeH3, FeH4, FeH6, FeH7 and FeQ2) gave first-order disappearance rate of TCE with tailing after 105 days of experiment that might be due to the accumulation of reaction products as previously reported by Miehr et al. (2004). For these irons, the last data point was omitted. For FeH1 and FeH9 slow or no reduction was observed and these data were assumed to be first-order rate. Rapid initial loss of PCE, TCE, cDCE and 1,1,1-TCA with no further reduction for FeH11 and FeH12 is due to the sorption properties as deduced from no detection of degradation products and no pressure build-up in batch reactors. To obtain disappearance rate constants, only first data were fitted and reported as a sorption. Similar was observed for FeH10 and FeH13 (PCE and TCE reduction), HQ (PCE reduction), FeS Aldrich (TCE reduction), FeS BIO1 (PCE, TCE, cDCE). FeS BIO2 showed slow degradation of PCE and 111TCA with tailing of TCE as a possible byproduct of PCE degradation and cDCE as a byproduct of TCE degradation. For this iron only first data for TCE and cDCE were fitted.

SI3. Change of pH and ORP values in time (days).

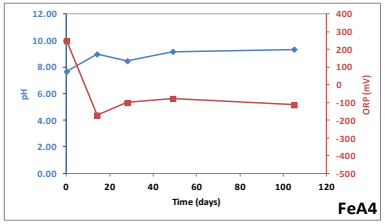

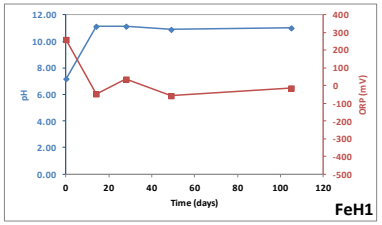

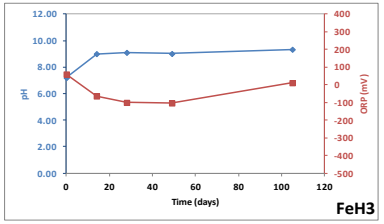

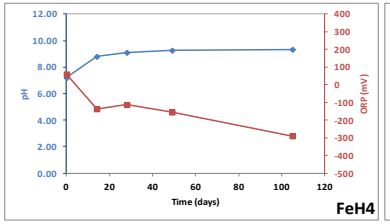

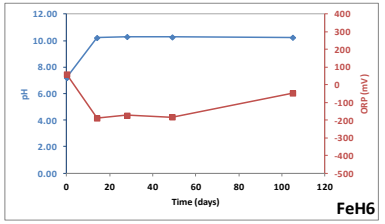

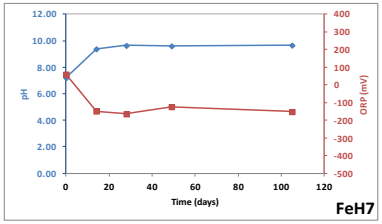

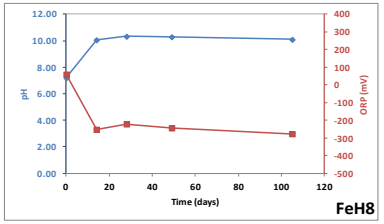

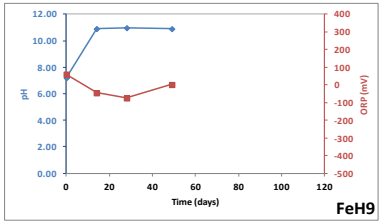

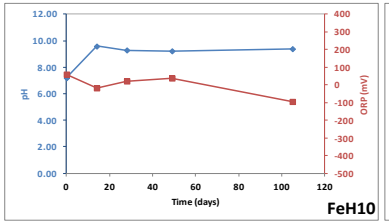

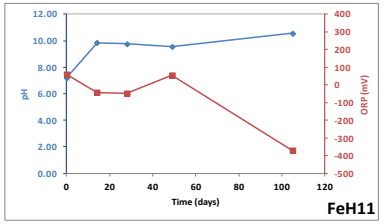

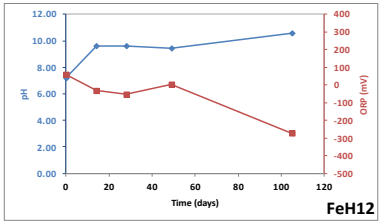

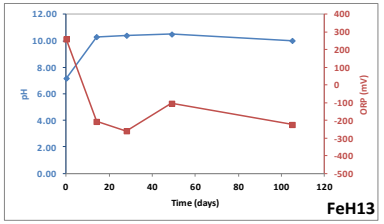

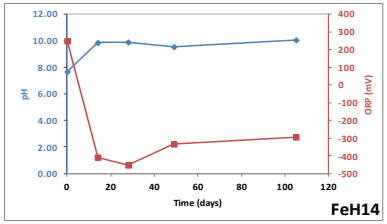

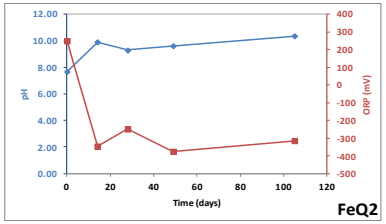

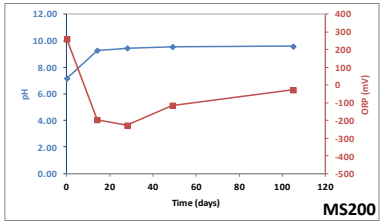

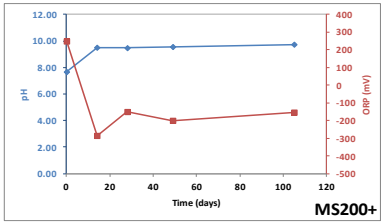

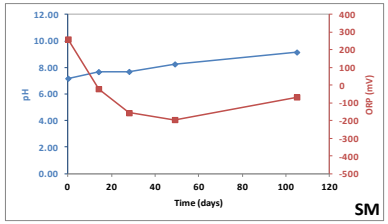

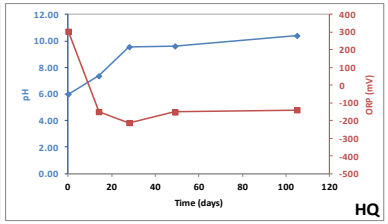

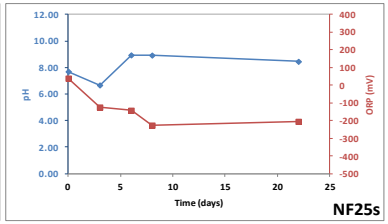

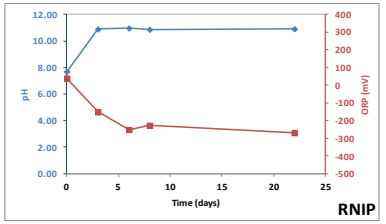

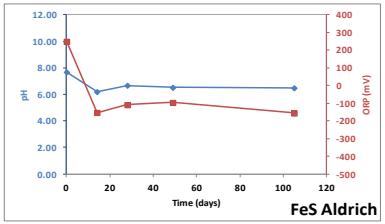

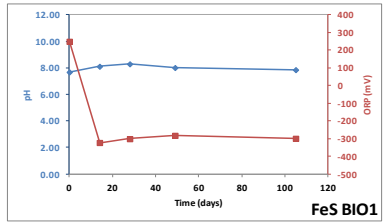

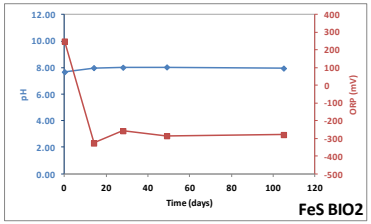

SI6. SEM images of several investigated microscale iron powders: (a) FeH4; (b) FeH7; (c) FeH8; (d) FeH12, (e) FeH13 and (f) BASF MS200.

SI7. Correlation between k_{obs} (h^{-1}) and iron particle size distribution D_{90} (µm) for all tested reactive materials.

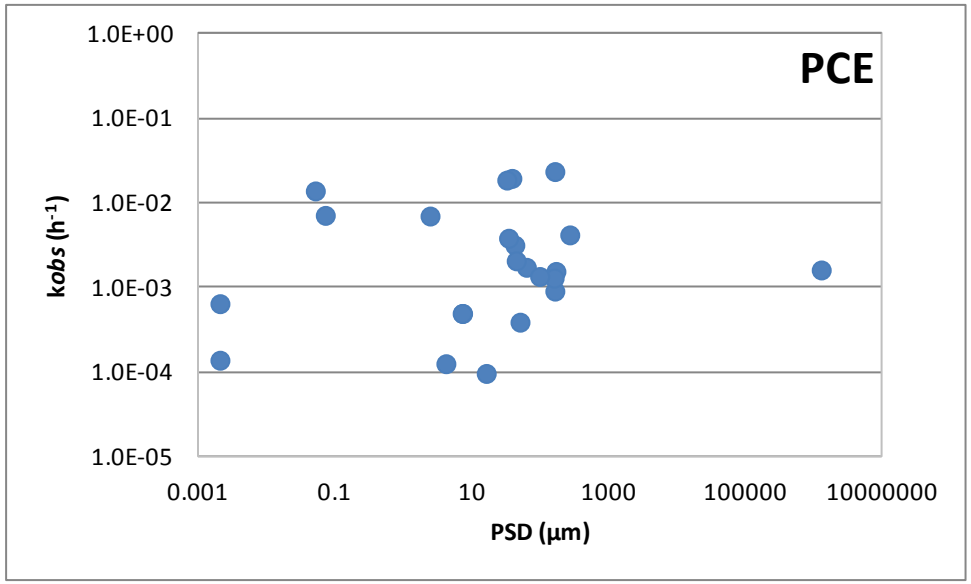

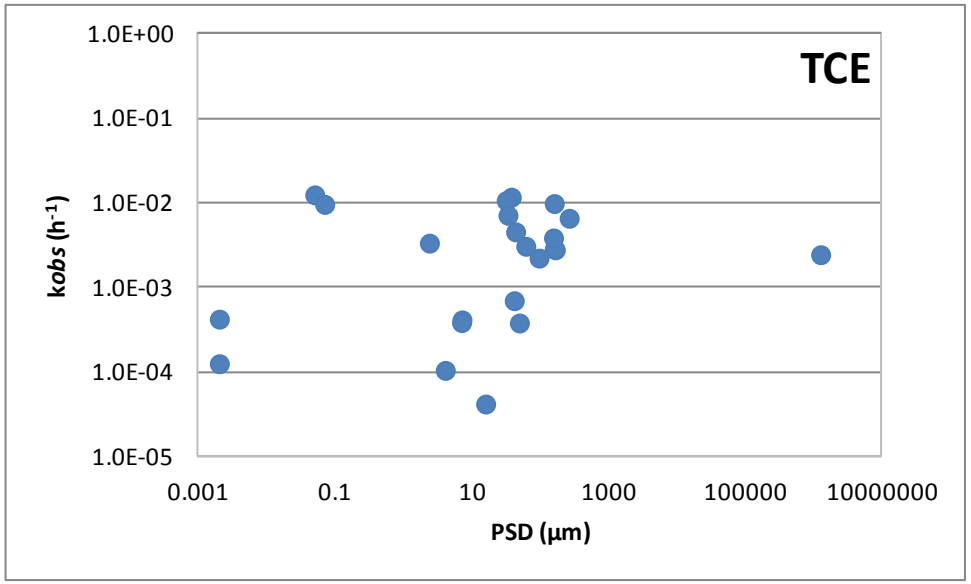

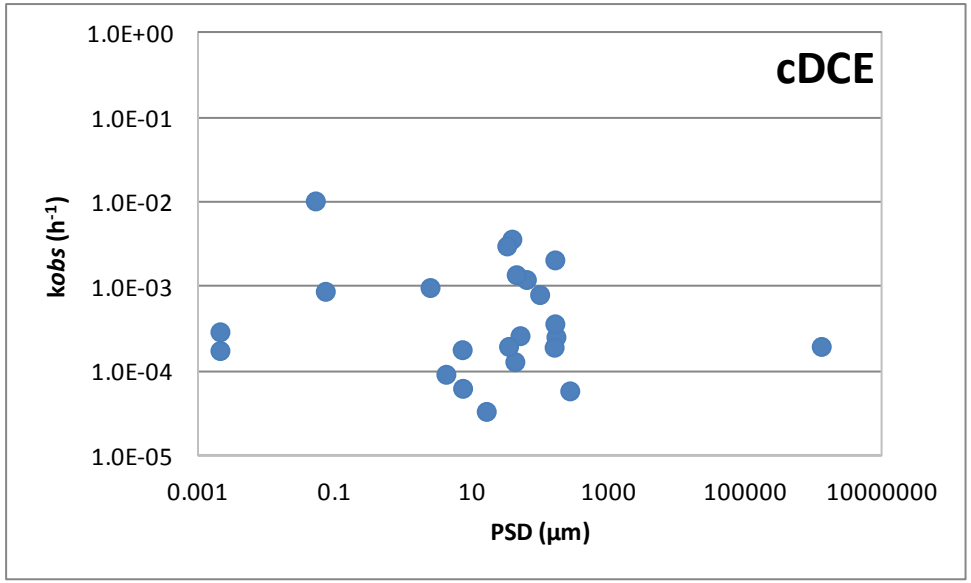

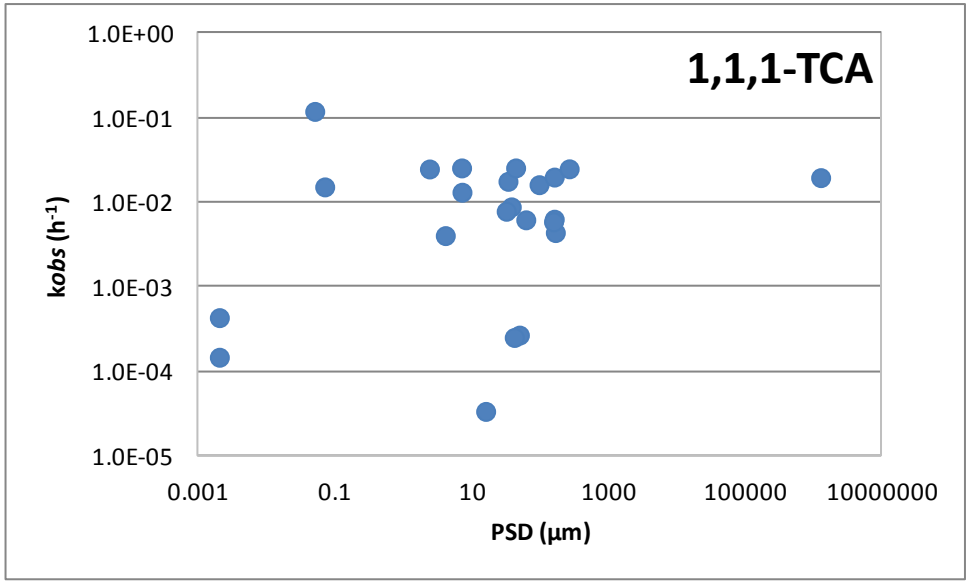

SI8. Reduction of 1,1,1-TCA by 50 g L^{-1} of FeH4 iron. Symbols are average concentrations from triplicate reactors.